DOI: 10.1111/risa.70004

ORIGINAL ARTICLE

Water outage predictions for natural hazards using synthetic water distribution systems

Zaira Pagan-Cajigas[1] | **Seth Guikema**[1,2] | **Rosalia Otaduy-Ramirez**[3] | **Vanessa Woolley**[4] | **Kaleb Smith**[5] | **Tongxing Hu**[6] | **Thomas Chen**[7]

[1]Industrial and Operations Engineering, University of Michigan, Ann Arbor, Michigan, USA

[2]Civil and Environmental Engineering, University of Michigan, Ann Arbor, Michigan, USA

[3]Knoxville Utilities Board, Knoxville, Tennessee, USA

[4]Anchor QEA, Baltimore, Maryland, USA

[5]Civil and Environmental Engineering, Cornell University, Ithaca, New York, USA

[6]Stantec, Los Angeles, California, USA

[7]Xylem Inc., Columbia, Maryland, USA

Correspondence
Zaira Pagán-Cajigas, Industrial and Operations Engineering, University of Michigan, Ann Arbor, MI, USA.
Email: zpagan@umich.edu

All co-authors were affiliated with the University of Michigan during the development of this paper. Their current affiliations may differ.

Funding information
One Concern Inc.

Abstract

Hazards can impact water systems, leading to water outages that result in economic, environmental, and societal losses. Modeling a system's behavior helps develop short-term restoration strategies and long-term resilience planning. However, data on the topology and operational characteristics of real water systems are often unavailable outside of the utility operating the system, limiting the ability of others depending on the system to understand its vulnerability and resilience. We address this limitation by developing an algorithm that generates a synthetic water distribution system using only publicly available data. Our approach provides hydraulic information at the building level to support infrastructure resilience assessments. We validated our model by comparing the network topologic and hydraulic properties with data from the real water system of Ann Arbor, Michigan. Our synthetic model results indicate that 95% of the simulated building-level pressures were within ± 25 PSI of the hydraulic model data from the existing system. To demonstrate an application of our model, we simulated water outages at the building level using hazard loading and fragility functions corresponding to an earthquake scenario.

KEYWORDS
outage estimation, synthetic water distribution systems, water outages prediction

1 | INTRODUCTION

Water distribution systems (WDS) are critical services (The White House, 2013), playing an essential role in ensuring a safe drinking water supply, which is vital for the population's health and well-being. Natural disasters can disrupt water supply, resulting in water outages that cause significant economic, environmental, and societal losses, as well as disruption to dependent critical infrastructures (American Society of Civil Engineers, 2021; Federal Emergency Management Agency, 2017; Toland & Wein, 2021). Although many hazards cause significant damage to WDS, these systems are particularly vulnerable to earthquakes (Environmental Protection Agency, 2018; Shi & O'Rourke, 2008).

Earthquakes can damage pipelines, tanks, and water treatment plants (WTP), resulting in low system pressures that cause long-term water service suspension (Environmental Protection Agency, 2018). Following an earthquake, a WDS often experiences longer downtime than the energy, gas, and communications systems (Kammouh et al., 2018). For instance, the 2014 magnitude 6.0 South Napa Earthquake severely impacted the City of Napa's WDS. It took seven days for water service to be restored to its pre-hazard capacity, while the energy and natural gas systems were restored within 24 hours (Earthquake Engineering Research Institute, 2014).

Water outage risk assessments assist utility companies, government agencies, emergency response facilities, and

This is an open access article under the terms of the Creative Commons Attribution-NonCommercial-NoDerivs License, which permits use and distribution in any medium, provided the original work is properly cited, the use is non-commercial and no modifications or adaptations are made.
© 2025 The Author(s). *Risk Analysis* published by Wiley Periodicals LLC on behalf of Society for Risk Analysis.

other utilities reliant on water services in developing short-term water restoration strategies and long-term resilience planning. In the short term, pre-event outage estimations enable water-dependent organizations to plan their response strategies more efficiently, reducing outage duration. Furthermore, pre-event risk estimation helps decision-makers allocate resources to improve post-hazard system performance. In the long term, estimating the likelihood of water outages at the building level allows water-dependent organizations to identify areas where additional redundancies and mitigation strategies should be implemented (Laucelli & Giustolisi, 2015).

Building-level outage estimates can help homeowners and businesses understand the potential impact of hazards on water availability, enabling them to build resilience at a local level. These estimates allow building owners to assess the potential benefits of preparedness and mitigation strategies such as backup water systems and downtime insurance policies. Additionally, these estimates assist community decision-makers in identifying areas most likely to be without access to adequate water service, guiding the allocation of alternative water supply sources, such as temporary storage tanks.

Researchers often use data from a real WDS to generate a virtual representation of the system, also known as a *digital twin*. This representation is used to assess hazard impacts and estimate the likelihood of water outages. However, data on the topology and operational characteristics are often unavailable for real WDS outside of the utility operating the system or are inaccessible due to security concerns (Mair et al., 2012, 2014; Möderl et al., 2011; Sitzenfrei, Fach, Kinzel, & Rauch., 2010; Sitzenfrei, Möderl, & Rauch, 2010; Sitzenfrei et al., 2013). The lack of data makes it difficult, if not impossible, to estimate building-level water resilience for those outside of the operating utility organization. Providing estimates at the building level using publicly available data would allow commercial entities, nonprofits, and other organizations outside of the local city government access to the potential benefits previously discussed.

Because of the persistent lack of publicly available data, researchers have developed virtual water distribution models (Ahmad et al., 2022; Mair et al., 2014; Möderl et al., 2011; Sitzenfrei et al., 2011; Sitzenfrei et al., 2013; Sitzenfrei, Fach, et al., 2010; Sitzenfrei, Möderl, et al., 2010). Virtual models vary in terms of network connectivity and complexity, as well as the number and types of water supply sources and their demand allocation models. Critically, these existing approaches are not intended to represent an existing water system. Instead, they are representations of potential systems. To date, virtual models do not provide strong support for mitigation and resilience planning for a real community.

To address these limitations, we developed a new approach that generates a synthetic water distribution system using only publicly available data, as well as a method for estimating water outages and pressure changes at a building level. This method develops a pressure-feasible synthetic system for existing communities, generalizable throughout the United States. This approach can simulate water outages caused by various hazards by adapting the fragility functions and hazard loading.

The remainder of this paper is structured as follows. First, we review previous research on virtual WDS generation and water outage estimation. We then introduce a new methodology for generating a synthetic WDS and simulating the impact of hazard loading on the system's performance. Then, we demonstrate the model's capability by validating the synthetic network layout and hydraulic properties against data from existing WDS. Finally, we simulate hazard loading scenarios on the synthetic system to evaluate the impact and location of water outages. The paper concludes with a discussion of the contributions and practical applications of our findings.

2 | LITERATURE REVIEW

Water systems are composed of transmission and distribution networks. The transmission system, consisting of large-diameter pipes, transports water from the source(s) to the WTP and through the various regions of the service area. The distribution system transports water from the transmission system to the demand points. The proposed framework generates a synthetic WDS, including both the transmission and distribution networks, to represent the layout and hydraulic behavior of the WDS and estimate outages at the building level. Our literature review examines previous methods for generating synthetic WDS, modeling their hydraulic behavior, and estimating post-hazard system performance.

2.1 | Layout model

Several methods have been developed to evaluate the impact of hazards on water systems and estimate the likelihood of water service disruption. Typically, these models use existing water systems' digital twins. Digital twins require precise geospatial, physical, and hydraulic information about the system components, such as pipe location, material and size, network connectivity, and tank and pump capacity. However, data limitations restrict the ability to estimate hazard impact to only those systems for which detailed data are available. This reduces the number of WDS for which we can currently evaluate pre- and post-hazard performance.

Additional research has focused on developing systematic models that generate a large number of virtual WDS (vWDS) by varying topological characteristics of existing systems, such as the number of assets, system structure, degree of connectivity, and water demand (Mair et al., 2014; Möderl et al., 2007, 2011; Sitzenfrei et al., 2013; Sitzenfrei, Fach, et al., 2010; Sitzenfrei, Möderl, et al., 2010). vWDS offer a large number of case study datasets, which are frequently used to test new hydraulic concepts and strategies. For example, Möderl et al. (2007) developed the modular design system (MDS). This graph theory-based approach automatically gen-

erates a vWDS by stochastically varying the system's layout structure, degree of connectivity, and water demand factors. However, the MDS model assumes a constant elevation along the components in the vWDS and is not intended to represent a specific system. Sitzenfrei et al. (2011) built upon Möderl et al. (2007) work and developed the WDS Designer. This model integrates the MDS graph theory approach with GIS data (e.g., population density and land use) to better represent the systems' water demand at the junction level. Furthermore, once the WDS Designer generates the water system layout, it is projected onto digital elevation maps to account for elevation variations in the water system. These systematic models help generate large case study datasets; however, the layouts are conceptual and only partially comparable to existing WDS because they do not accurately approximate topology. Spatially explicit models of existing WDS incorporate data about components' spatial distribution and their interaction. These models are crucial for supporting outage estimations and resilience planning for water utilities; however, they are rarely available.

Open-source digital maps (e.g., OpenStreetMap) and surrogate data sources (e.g., street networks) are an alternative to gathering accurate spatially explicit information on the WDS topology (Haklay & Weber, 2008; Logan et al., 2019; Mair et al., 2012). These digital maps are geographic repositories that identify overground infrastructure locations and characteristics (e.g., street classification) (Haklay & Weber, 2008). To our best knowledge, although there has been research on the coverage of building data, which includes WTP, indicating a 64% coverage in North American urban areas (Herfort et al., 2023), no research has specifically focused on analyzing the coverage of overground WDS components within these digital repositories. Furthermore, data on the location of underground water infrastructure, including pipes, valves, and pumps, are limited (Yu et al., 2021). While maintenance holes ("manholes") provide spatial insight into the underground WDS layout, gathering this information for large systems is time-consuming and complex.

A more accurate representation of component locations is essential to estimate water outages following a hazardous event. To address the lack of spatially explicit data for underground components, Mair et al. (2012) examined the intersection between publicly available street data and water networks (Mair et al., 2012, 2017). The findings revealed a strong correlation between street and water system layouts, particularly in urban areas. As a result, researchers began to use street network data as a proxy for WDS (Ahmad et al., 2022; Mair et al., 2014). For example, Mair et al. used a spanning tree algorithm that inputs street data to generate synthetic WDS (Ahmad et al., 2022; Mair et al., 2014). However, it does not generate a realistic hydraulic model, as junction pressure estimates are based exclusively on pressure surface maps.

Other recent approaches provide more realistic hydraulic models by using publicly available data but fail to incorporate demand estimates at a sufficiently fine spatial scale (e.g., building level). For example, Ahmad et al. (2022) developed the synthetic infrastructure model (SyNF), which generates synthetic water systems based on street data, population density, and water source locations. However, their demand model evenly distributes estimates of monthly water demands across all nodes in a census block. As a result, homogenized demand estimates fail to capture demand variations within the census block. Building-level demand estimates provide more realistic representations of the system's demand patterns.

2.2 | Hydraulic model

Various hydraulic modeling software tools have been developed to simulate the hydraulic behavior of a water system following a natural hazard event. These tools use mass and energy conservation equations to model the system's water flow and pressure changes. Commonly used approaches for modeling the hydraulics of WDS include demand-driven analysis (DDA), quasi-pressure-driven analysis (quasi-PDA), and pressure-driven analysis (PDA).

DDA simulators assume the consumer's demand must be fully satisfied regardless of the nodal pressure and flow. This approach is adequate under normal operating conditions where the system's hydraulic pressure is sufficient to supply all required demands regardless of the nodal pressures (Laucelli et al., 2012; Wu et al., 2008). However, in many damage scenarios, such as pipe breaks or pump failures, the system may not be able to supply the required demand, resulting in negative pressures (Muranho et al., 2020). EPANET is a widely used DDA simulator (Rossman et al., 2020). However, some EPANET extensions (e.g., EPANET2) account for low operating pressure conditions by using Quasi-PDA simulators (Pathirana, 2011).

Quasi-PDA simulators suppress the occurrence of negative pressures by iteratively running DDA simulations until there are no negative pressures in the system. Based on the simulation's demand and pressure results, the nodes' conditions are switched between fixed, reduced, or zero demand in each iteration (Pathirana, 2011; Yoo et al., 2016, 2017). The Graphical Iterative Response Analysis for Flow Following Earthquakes (GIRAFFE) tool incorporates various types of pipe breaks and leaks into its damage simulation (Cornell University, 2008). GIRAFFE employs a quasi-PDA simulator to remove negative pressure from the damaged system iteratively, along with their associated links and control parameters (Romero et al., 2010; Wang, 2006; Wang & O'Rourke, 2007).

PDA simulators assume the supplied consumer demand is a function of nodal pressure (Wagner et al., 1988). This method specifies a minimum pressure threshold below which no water is supplied and a base pressure threshold above which all water demand is met. Nodes with pressure between the minimum and base pressure are assumed to receive a reduced water supply quantity (Laucelli & Giustolisi, 2015). PDA simulators are widely used because of their ability to simulate pressure-deficient conditions caused by increased demands, pipe leaks or breaks, and pump failures (Cheung et al., 2005; Fujiwara & Li, 1998; Germanopoulos, 1985; Giustolisi et al., 2008; Laucelli et al., 2012; Wu et al., 2008). Some examples of PDA simulators include WaterGEMS (Laucelli et al.,

2012; Muranho et al., 2012), an open-source simulator that allows for modeling volume-based and pressure-dependent demand, and WaterNetGen, a commercial simulator that performs a pressure-driven analysis while accounting for pipe leakage (Muranho et al., 2012, Muranho et al., 2014).

Recent modeling software tools integrate a flexible interface that allows users to choose between multiple hydraulic approaches and even change the approach during the simulation. For example, the Water Network Tool for Resilience (WNTR) is an open-source Python package that simulates the network hydraulic operations using EPANET's DDA simulator or an internal PDA simulator (Klise, Bynum, et al., 2017; Klise, Hart, et al., 2017; Klise et al., 2018). Our approach integrates WNTR to generate our hydraulic model, which allows for flexible controls to change the status and operations of the system's components and allows us to simulate the system's hydraulics with a DDA or PDA simulator.

Hydraulic models provide valuable pressure data, which can be used to establish pressure zones. Pressure zones are semi-independent hydraulic subdivisions that maintain a minimum and maximum pressure range with few to no additional control equipment. Failing to account for these pressure zones in a model can result in inaccurate pressure estimates, especially in areas with significant elevation changes. Modeling pressure zones allows for parallelization of the model, which reduces the computational burden, particularly in larger water systems.

2.3 | Damage model

Research estimating water outages mostly focuses on evaluating the WDS performance after an earthquake. Compared with other hazards, earthquakes cause the most significant damage to WDS. Peak ground velocity (PGV) and peak ground acceleration (PGA) attenuation models are commonly used to establish the relationship between ground movements and the damaged state of components. PGV models assess the damaged state of the pipelines by directly relating it to the earthquake's longitudinal ground strain (Romero et al., 2010). Damage models frequently incorporate the pipe repair rate and PGV to estimate the damage state for each pipe (American Lifelines Alliance, 2001b). PGA attenuation models are commonly used to model the damage state of above-ground components, such as pumps, tanks, and WTP (Klise et al., 2018).

Empirical fragility curves are widely used to describe a component's probability of reaching or exceeding a damaged state due to hazard loading. These curves are hazard- and component-specific, meaning a component's likelihood of reaching a specific damage state is determined by the type and intensity of the hazard as well as the component's characteristics (e.g., material and size). For example, a fragility curve can provide the probability of a PVC pipe experiencing minor leaks, major leaks, or breaks, given a specific hazard loading.

To estimate individual building-level water outages, fragility curves alone are not sufficient. Instead, component-level damage estimates are used to simulate the hydraulic behavior of the WDS. The Monte Carlo simulation method is commonly used to generate replications of each component's damaged state. For each replication, the hydraulics are modeled to evaluate water flow and determine building-level water availability. These results are used to estimate water outage location and duration, which is valuable for developing effective mitigation, preparedness, and recovery strategies.

WNTR uses fragility functions to model earthquake effects on the WDS. This tool includes various PGV and PGA models to account for differences in local geology. The fragility assessments of the tanks and pumps are determined using three PGA attenuation models, while two PGV attenuation models are utilized to calculate the pipe repair rate (Baag et al., 1998; Kawashima et al., 1985; Lee & Cho., 2002). Failure and leakage probability equations are derived from the damage probability equations developed by the American Lifelines Alliance (ALA, 2001b).

3 | MODEL DEVELOPMENT

3.1 | Assumptions and information needed

Our methodology relies on open-source data to generate the synthetic WDS. The required data include WDS boundaries, building and key component locations, ground elevation, and road network information. The WDS boundaries are publicly available for 24 states and the District of Columbia (McDonald et al., 2022). Moreover, a national dataset was created by the Environmental Policy Innovation Center in collaboration with SimpleLab (Environmental Policy Innovation Center, n.d). This dataset includes WDS boundaries obtained directly from states or utility companies and boundaries estimated based on population and water supply facility locations.

Elevation data are available from the USGS 3D elevation dataset, which provides shapefiles with contour lines for all cities in the United States (Stoker & Miller, 2022). Considering elevation variations in the WDS is crucial to represent the system's hydraulic behavior, as elevation changes can impact the pressure head. In this context, assuming ground elevation as a proxy for asset elevation is a reasonable approach.

Another critical input is the location of the water supply infrastructure, such as WTP(s) and storage tanks. The locations of these components are publicly available for most US cities through open-source platforms such as OpenStreetMap (OSM) (Haklay & Weber, 2008). For our case study community, we utilized tags such as "water_works" for identifying WTP(s), and "water_tower" and "storage_tanks" with "content = water" for storage tanks. Additionally, we cross-verified the location of WTP(s) using satellite imagery and mapping data from Google Maps and on-site validation. Furthermore, we corroborated tank locations by comparing results to data provided by the local utility company. For our case study sites, the data exported from OSM was accurate; however, careful consideration and verification should still be

performed for other locations, as OSM data reliability can vary.

Our approach uses publicly available data from other infrastructure systems as a proxy to develop the WDS layout. Building location and use classification data are obtained from building footprints which are accessible for most US cities through municipal databases. We assume every building in an urban setting in the US receives water service. Thus, we approximate the location of water meters using building locations. However, in some cases, there may be multiple water meters per building, but we do not consider this in our approach. We utilized building use classifications to estimate daily water consumption patterns. This accounts for differences in water consumption between consumer types. For example, a large industrial user's hourly water consumption pattern differs from that of a residential user.

Some crucial assumptions underlying our approach for generating a synthetic WDS are:

1. The pipeline network is primarily developed along the road network.
2. There are no pipelines under interstates, highways, or ramps.
3. Major road arterials are a proxy for water mains.
4. An unlimited water supply is available from the WTP(s) into the distribution system (e.g., we do not consider drought or other low-supply situations). This could be included in a future extension of the method.
5. The network is a combination of loop and radial structure.

As previously discussed, one of our fundamental assumptions is that the pipeline network is primarily developed along roads. This assumption is based on empirical evidence from Mair's case studies, which indicate that approximately 80% of the WDS are within 50%–78% of the road network (Mair et al., 2012, 2017). These findings suggest a strong correlation between the two networks. However, to ensure full connectivity in our system, additional pipes may also be strategically located along junctions. The road layouts are publicly available at the county level from the United States Census Bureau.

Based on previous communications with water utilities, utilities avoid situating pipelines along these critical roads as pipeline damage may significantly disrupt traffic flow. For this reason, we assume there are no pipelines under roads classified as interstates, highways, or ramps. Given the common practice that utilities place larger-diameter pipes along major arterial roads, we assume water mains are situated along these roads.

Our synthetic model accounts for both looped and branched sections in the WDS. According to previous investigations (Mair et al., 2017), 88% of the system consists of looped sections, while the remaining 12% are branch sections. Additionally, they determined that loop sections are more prevalent in urban areas, while branched sections are more commonly found on the city's periphery.

Furthermore, our synthetic WDS model does not account for every component in the real system. Instead, it focuses on the infrastructure frequently impacted by natural hazards and whose failures commonly result in water outages. These components include WTP, tanks, pumps, and pipelines. The extent of system damage and impacted components depends on the type and intensity of the hazard.

3.2 | Network generation methodology

Section 3.2 outlines the methodology for generating a synthetic WDS, which includes two main models: the layout model and the hydraulic model. The layout model generates the system's layout by selecting the WDS's nodes and edges, along with their respective locations and interconnections. Subsequently, the hydraulic model determines the hydraulic properties of the components and models the system's hydraulic behavior.

3.2.1 | Layout methodology

To generate the WDS layout, we followed an eight-step process, as shown in Figure 1.

First, we create a node–edge graph using road data (Step 1a), where nodes are located at road intersections and edges represent connections between nodes following the road network. Then, the graph is pruned by removing parallel edges, linked to the same two nodes. Subsequently, each edge is categorized according to its road classification, with major arterial roads classified as water mains and local roads as potential distribution lines (Step 1b).

Next, building location data are used to calculate the Euclidian distance between every building and node in the system; each building is assigned to the nearest node (Step 1c). Nodes with assigned buildings are classified as demand nodes. These nodes are required to supply the aggregated demand of their assigned buildings (Step 1d). The following steps select water main demand nodes (Step 1e) and link the unconnected water main nodes to the largest connected graph component (Step 1f). This process uses the shortest path algorithm following the edges, considering only water main nodes; this step is repeated until all the main water nodes are connected. The remaining demand nodes are then added to the distribution lines (Step 1g).

Finally, the WTP(s) and tanks are incorporated into the system and connected to the water mains using the shortest path algorithm (Step 1h). The layout model outputs the locations of nodes, the buildings attributed to each node, and the network connectivity for the WDS layout.

3.2.2 | Hydraulic methodology

After generating the WDS layout, the hydraulic model uses the WNTR software to generate the hydraulic system. The

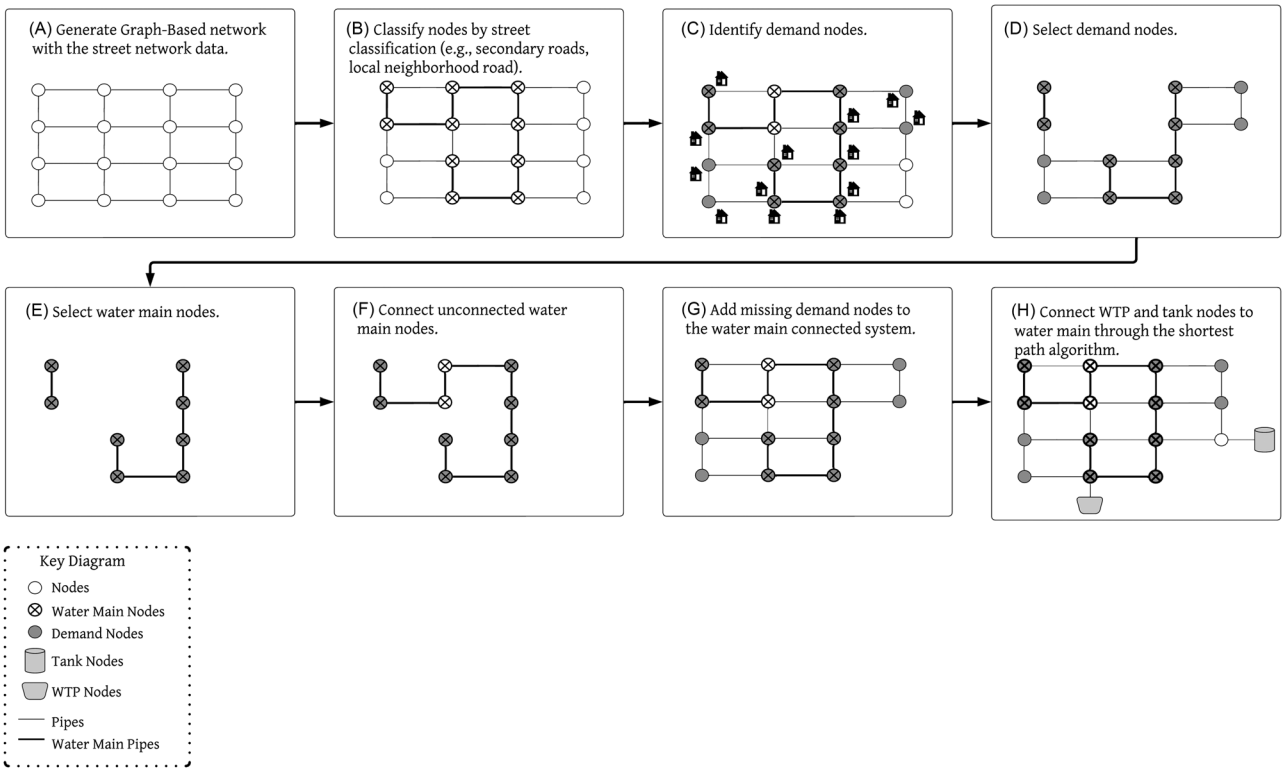


FIGURE 1 Layout model flowchart.

methodology for this model is subdivided into three sections, as shown in Figure 2. The first section generates an initial hydraulic system to estimate nodal pressures without accounting for pressure zones. The second section uses these pressure estimates to allocate the nodes into pressure zones and create individual hydraulic subsystems. The third section generates a merged system by connecting all pressure zones at the WTP level, maintaining the hydraulic properties of the individual subsystems. Either the individual subsystems or the merged system can be used as inputs for the damage model.

Generate the initial hydraulic system

Step 2a. Add junctions. This section describes the initial setup of the hydraulic system without accounting for pressure zones. The first step, 2a, integrates the junctions into the initial WNTR hydraulic system and assigns their daily water demand pattern. These junctions correspond to the nodes from the layout model output. Each junction contains a set of attributes, including unique identifiers, geographic coordinates, base demand, daily demand patterns, and elevation.

The unique identifier and geographic coordinates are obtained from the layout model output. The base demand for each junction is set to 300 gallons of water per day, corresponding to the daily average household water consumption in the US (Environmental Protection Agency, 2008). Each daily demand pattern, structured as a 24-dimensional row vector $(v_1, v_2, v_3, \ldots, v_{24})$, represents hourly water consumption. Our hydraulic model includes ten daily demand patterns, one for each building use classification, including small, large, and multi-unit residential, commercial, hospitality, medical, irrigation, retail, office, and larger users.

We evaluate the use classification of each building assigned to each node to calculate the daily demand pattern at the junction level. If only one building is assigned to the node, the daily demand pattern is set to that of the building. If multiple buildings are assigned to the node, the algorithm aggregates all demand patterns into a single *total daily demand* for that junction. Additionally, the elevation for each junction is based on data from the USGS elevation database.

Step 2b. Add pipes. Step 2b incorporates pipes into the initial WNTR hydraulic system, which correspond to the edges from the layout model output. Each pipe includes a set of parameters, such as the start and end coordinates, length, diameter, roughness, and initial status.

The coordinates and length are obtained from the layout model output. The pipe diameters are determined based on the edge classification. Pipes connecting tanks to water mains are assigned a diameter of 30 inches. Water main pipes are assigned a diameter of 16 inches, and all other pipes are assigned a diameter of 6 inches. Additionally, our model includes a pipe dictionary with multiple materials such as PVC, steel, ductile iron, and concrete. The choice of pipe material is a manual input and can be modified to reflect the specific requirements and characteristics of the WDS under analysis. The roughness coefficient, which affects the flow characteristics of the pipe, is determined by the pipe's mate-

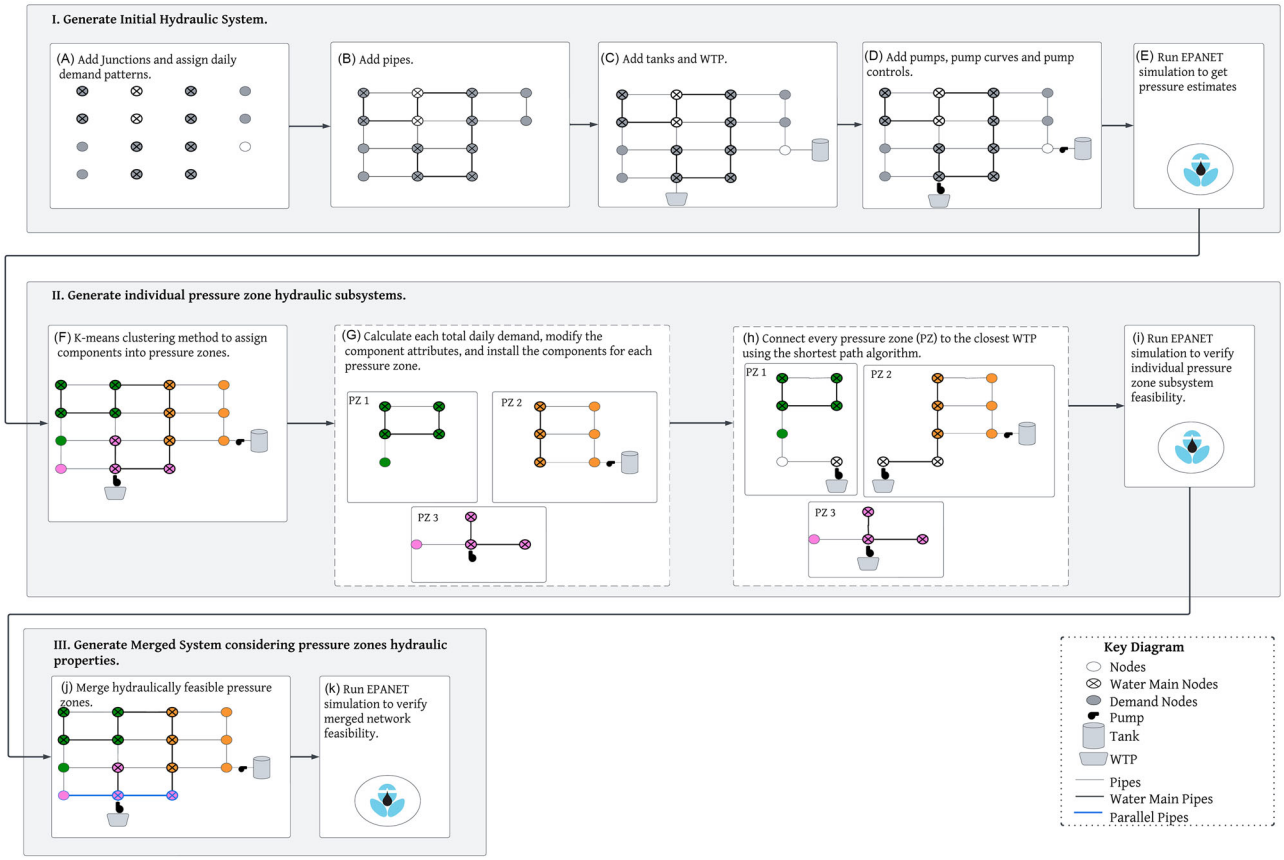


FIGURE 2 Hydraulic model flowchart.

rial (American Lifelines Alliance, 2001b). Finally, the initial status for each pipe is set as "OPEN," indicating that water can flow through the pipe.

Step 2c. Add storage tanks and WTP(s). In step 2c, the model incorporates the storage tanks, which are critical for pressure management and water storage. This step requires the tanks' coordinates, ground elevation, base elevation, head, diameter, volume, and initial/maximum water levels.

The ground elevation for each tank is based on data from the USGS elevation database. The tanks' base elevation depends on whether they are classified as ground or elevated tanks, determined by their daily water demand. In the initial hydraulic system, the daily demand for each tank is calculated by distributing the total daily demand equally among all tanks. In this section and subsequent sections, tanks with a daily demand of less than one million gallons are classified as elevated; those with greater demands are classified as ground tanks. To maintain a minimum system pressure of over 25 PSI, the base elevation of elevated tanks is increased by 18 meters.

The head required to achieve 25 PSI is calculated using a simplified version of Bernoulli's law, as presented in equation (1).

$$h = \frac{p}{\rho g}. \tag{1}$$

The variable h represents the minimum head required to maintain the desired pressure, p is the minimum desired pressure (25 PSI), ρ represents fluid density, and g is the gravitational acceleration.

The tank diameter is determined according to industry sizing guidelines for double ellipsoid and elevated toro tanks (Pittsburg Tank & Tower Group, n.d.). These guidelines provide a correlation between the tank's total daily demand and its diameter.

The tank volume is equivalent to the sum of the equalizing, fire flow, and operational storage. Equalizing storage acts as a buffer to support water demand fluctuations and supplement the WTP(s) steady water supply rate. Meanwhile, fire flow storage is reserved for firefighting purposes. Operational storage is intended to meet the system's water demand. Assuming a cylindrical shape for the tanks, we determined each tank's height by applying the formula for the volume of a cylinder, solving for height. The calculated height represents the initial and maximum water level for each tank, in other words, tanks start the simulation at maximum operational storage conditions.

In step 2c, the model also incorporates the water treatment plants into the WNTR hydraulic system, which requires data on the WTP(s) coordinates and elevation. The elevation for WTP(s) is obtained from the USGS elevation database. In this model, the WTP(s) are assumed to have an infinite water sup-

ply; however, this assumption can be modified to reflect more restrictive water supply conditions, such as those experienced during drought conditions.

Step 2d. Add pumps, pump curves, and pump controls. In Step 2d, the model generates pump curves and integrates pumps into the hydraulic system. In this initial system, pumps are placed exclusively from the pipes into the elevated tanks. A standardized single-point pump curve is assigned to each pump, based on the pressure head (H) and flow rate (Q) of the tank. The pressure head reflects the vertical distance between the tank's maximum water level and the ground, which is considered the discharge point in our model. The flow rate (Q) is calculated using equation (2), which considers the volume of the tank associated with the pump:

$$Q = \frac{V}{3}. \tag{2}$$

In this model, the pump controls are configured to activate (open) the pump when the tank's volume drops below a predetermined threshold, set at the combined capacities of the equalizing and fire flow storages. The pump continues operating until the water level reaches the specified upper shut-off limit, which is set to the tank's maximum height.

Step 2e. Run EPANET simulation. After completing the initial hydraulic system, the model runs a DDA EPANET simulation that generates head and pressure data for all nodes in the system (2e). To ensure the data are reliable, we removed a 24-hour burn-in period to eliminate the effects of the assumed initial conditions of the system.

Generate an individual hydraulic subsystem for each pressure zone

Step 2f. K-means clustering algorithm. This section describes the method for generating a hydraulic subsystem for each pressure zone. In Step 2f, the model allocates junctions, pipes, tanks, and pumps into their respective pressure zones. This process uses a K-means clustering algorithm, which groups junctions into distinct clusters based on their geographic location and initial pressure estimates. These pressure estimates are obtained from the initial simulation results (Step 2e). The number of clusters, corresponding to the number of pressure zones in the system, is a manual input. For our case study, we acquired these data from the City of Ann Arbor Water System Master Plan.

Pipes are assigned to a pressure zone based on the geographic location of their start and end junctions; the pipe is assigned to the zone if both junctions are located within the same zone. Tanks are allocated to a pressure zone based on the most frequent zone classification of junctions within a half-mile radius of each tank. Lastly, pumps are assigned to the same pressure zone as their associated tank.

Step 2g**. Calculate total daily demand and install components in each pressure zone**. In Step 2g, the model calculates the daily demand for each pressure zone by aggregating the demand patterns of the junctions assigned to it, as described in Section 1. It then updates and installs the attributes of each component within the zone to ensure that they are calibrated to meet the specific demand requirements of that zone.

The model distributes the aggregated demand among the tank(s) within the zone. If no tank is assigned to the zone, the demand is allocated to the nearest WTP. For zones with multiple tanks, the demand allocation depends on the tank's classification, with ground tanks receiving a larger proportion of the total demand, following a 2:1 ratio compared with each elevated tank.

Following demand allocation, the model recalculates the volume, diameter, and height of each tank based on the updated assigned demands, as described in Section 1. Pump curves are then redefined for each pump, utilizing the revised pressure head (H) and flow rate (Q) from tanks. This process involves recalculating the single-point pump curve for each pump based on the updated tank attributes. Once all components are updated, the model proceeds with the installation of these components, following the procedures described in Section 1.

Step 2h. Connect every pressure zone to the nearest WTP. Finally, Step 2h integrates the WTP(s) into the pressure zones. This is achieved by establishing a direct connection between the pressure zones' water mains and the WTP, using the shortest path algorithm. The connecting pipes are assigned a diameter of 30 inches. This step may require installing additional junctions and pipes into the pressure zone. In such cases, the new junctions are classified as transitional junctions as they do not directly supply water to the zone.

Step 2i. Run DDA simulation. After generating a separate hydraulic subsystem for each pressure zone, the model performs a DDA EPANET simulation to verify the hydraulic feasibility of each subsystem (2i). This step verifies that our synthetic system maintains realistic pressures under normal operation conditions. If the system fails to meet the required pressure feasibility, the algorithm resizes the pipes to meet the feasibility.

Generate a merged hydraulic system

Steps 2j and 2k. Generate a merged hydraulic system and run a DDA simulation. This final section combines all pressure zones into a single hydraulic system, maintaining each zone's hydraulic properties (2j). In this merged hydraulic system, all zones are interconnected at the WTP level to better replicate real-world WDS hydraulic behavior. Once the system is merged, the model performs a DDA EPANET simulation to verify hydraulic feasibility (2k), as in Step 2i. Depending on the size of the system and the computational capability, the user can either use the single hydraulic subsystem or the merged hydraulic system for subsequent analysis.

3.3 | Damage model

The damage model simulates the impact of an earthquake on our synthetic WDS and evaluates the building-level likeli-

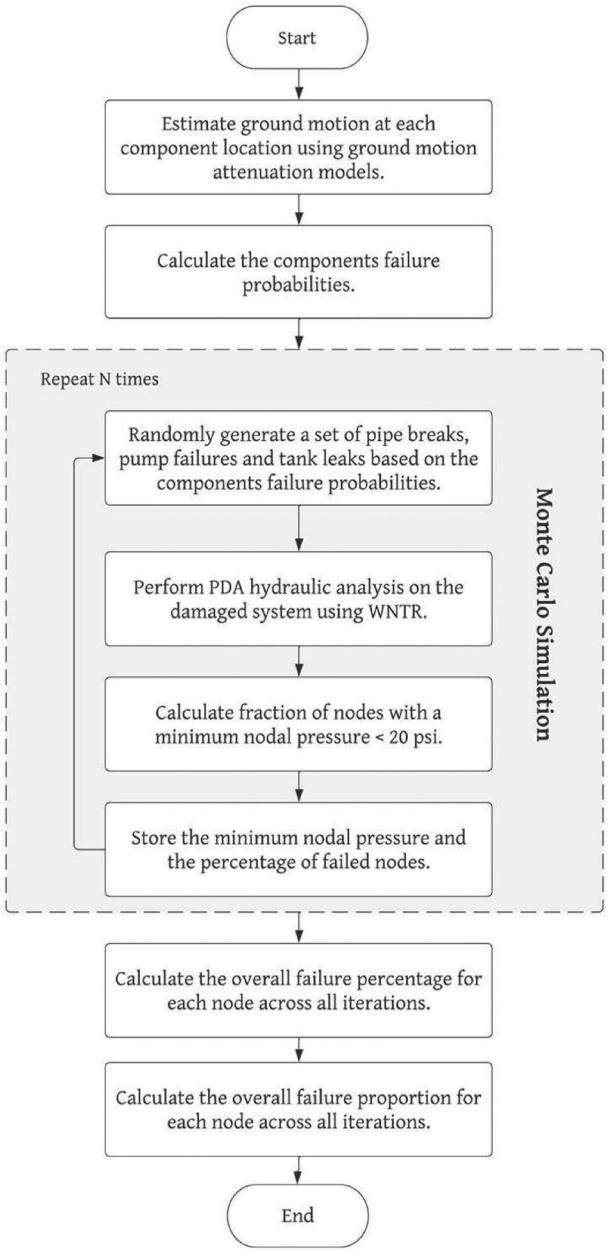


FIGURE 3 Damage model flowchart.

hood of losing water service post-hazard. The damage model methodology is shown in Figure 3.

3.3.1 | Earthquake attenuation model

The damage model incorporates attenuation equations to represent the propagation of seismic waves. These equations quantify the attenuation of seismic waves at a specific geographic location using PGA and PGV equations. Our model includes multiple PGA and PGV equations to account for site-specific characteristics.

The tank and pump damage estimates are calculated by averaging the empirical equations presented in Kawashima et al. (1985) and Lee and Cho (2002):

$$PGA = 403.8 \times 10^{.265M}(R+30)^{-1.218}, \tag{3}$$

$$log\,(PGA) = -1.83 + 0.386M - log\,(R) - 0.0015R. \tag{4}$$

In this equation, PGA represents the peak ground acceleration in $\frac{cm}{s^2}$, M represents the earthquake's Richter scale magnitude, and R represents the distance from the epicenter to the centroid of the component in km.

Similarly, our model estimates pipe damage by averaging Yu and Jin's (2008) PGV equations for rock and soil:

$$PGV_{rock} = 10^{0.848+0.775M+1.834(R+17)}, \tag{5}$$

$$PGV_{soil} = 10^{-0.284+0.711M+1.85(R+17)}, \tag{6}$$

where PGV represents the peak ground velocity in $\frac{cm}{s}$ and R represents the distance from the epicenter to the midpoint of each pipe in km. The resulting averaged PGV value is then used to calculate the seismic pipe repair rates.

3.3.2 | Component-specific fragility functions

The seismic pipe repair rates are calculated using the ALA equations (American Lifeline Alliance, 2001a, 2001b):

$$RR = (K \times 0.00187 \times PGV), \tag{7}$$

where RR represents the seismic repair rate per 1000 feet of pipe, and K represents the fragility curve modification factor based on the pipe material, diameter, joint, and soil corrosivity. Equation (7) is then modified to estimate the repair rate for a single pipe (RR_i) [equation (8)]:

$$RR_i = (K \times 0.00187 \times PGV) \times \frac{(L)}{1000}, \tag{8}$$

where L is the pipe length in ft. The Poisson equation proposed by the ALA (American Lifelines Alliance, 2001b) uses the component-level repair rates to calculate the probability of failure for each pipe [equation (9)]. Given a failure, the breaks are applied to the pipe's midpoint.

$$P_{failure} = 1 - e^{-RR}. \tag{9}$$

3.3.3 | Pressure-driven simulator

Conventional DDA simulators assume the demand at each node is always met, which is not realistic in damaged WDSs. Therefore, a PDA simulator is necessary to account for pressure-deficient scenarios caused by various factors, such as increased demand, supply reduction, or system failures. Our model incorporates the WNTR PDA simulator proposed by Wagner et al. (1988), which utilizes equation (10) to establish the relationship between pressure and the demand delivered to a node.

$$d_i = \begin{cases} 0 & p_i < P_0 \\ D_f \sqrt{\frac{p_i - P_0}{P_f - P_0}} & P_0 \le p_i \le P_f \\ D_f & P_f \le p_i \end{cases} . \tag{10}$$

In this equation, d_i represents the demand delivered to node i, D_f represents expected demand, p_i represents the pressure at node i, P_f represents the pressure threshold above which node i receives the expected demand, and P_0 represents the pressure threshold below which node i is not supplied water. In our model, P_0 and P_f are 0 and 20 PSI, respectively.

3.3.4 | Resilience metric

Our model estimates the probability of a building experiencing insufficient water pressure. For this, we modified the equation proposed by Klise et al. (2017) to identify failed nodes in the system [equation (11)]. A node fails at time t if its pressure drops below the minimum pressure (τ) required for supporting fire flow, which is associated with an increased risk of boil water notices. In our analysis, the threshold τ is equivalent to 20 PSI:

$$n_i = \begin{cases} 1 & p_i < \tau \\ 0 & otherwise \end{cases} . \tag{11}$$

In equation (11), the binary variable n_i is defined as 1 if node i experiences pressure below the threshold τ, and zero otherwise. For each iteration, the model stores the buildings experiencing insufficient water pressure, which are those assigned to the failed nodes, and calculates the proportion of impacted buildings (BI), using equation (12):

$$BI = \frac{\sum_{i \in I} b_i n_i}{\sum_{i \in I} b_i}, \tag{12}$$

where b represents the total number of buildings receiving water supply from node i, and I represents the total number of nodes in the WDS.

3.3.5 | Monte Carlo simulation

A Monte Carlo simulation is used to address uncertainties associated with hazards impacting WDSs. For each iteration of the Monte Carlo simulation, pipe breaks, reservoir failures, and pump failures are generated based on the component's fragility functions. The resulting damaged system is then subjected to the WNTR PDA simulator. The pressure results are used to identify nodes experiencing pressure below the threshold τ, as described in Section 3.3.4. The process is repeated for a predetermined number of iterations based on convergence to a 95% confidence interval and an error rate of 0.05. The minimum nodal pressure and the fraction of failed nodes for each iteration are stored to calculate the probability of buildings experiencing insufficient water pressure and the proportion of impacted buildings across all iterations.

4 | EXAMPLE DEMONSTRATION

4.1 | Case study

This section demonstrates an implementation of the layout, hydraulic, and damage models with a case study of the city of Ann Arbor, Michigan. This city was chosen because the utility company provided a digital twin and data on minimum, maximum, and average daily pressures from the existing WDS, which allowed us to validate our synthetic WDS layout and pressure results. For the remainder of the paper, we will refer to the digital twin utilized by the utility company as the "real system," while acknowledging that there may exist variances between the digital twin and the physical system.

As of 2021, Ann Arbor has a population of approximately 121,500 people and 25,000 buildings. Ann Arbor's existing WDS layout is presented in Figure 4A, consisting of one reservoir, one treatment plant, seven tanks, 101 valves, 25 pumps, 14,776 junctions, 16,136 pipes, and serves approximately 118,000 consumers. Our synthetic WDS layout is presented in Figure 4B, consisting of one reservoir, one treatment plant, seven tanks, seven pumps, 4642 junctions, and 4859 pipes. Valves, including pressure-reducing valves (PRVs), are not included in our network model. However, we acknowledge that the omission of this component can present challenges when aiming to simulate a system located in an area with high elevation differences.

Our synthetic WDS has fewer nodes and edges than the existing WDS as it does not include pipes connecting the distribution system directly to buildings. Instead, our model assigns each building to the nearest node in the distribution system. Furthermore, the existing WDS has more redundancy due to the removal of self-loops in our synthetic WDS. Our focus is not on replicating the exact topology of the system, but on estimating building-level pressure under normal and disruptive conditions.

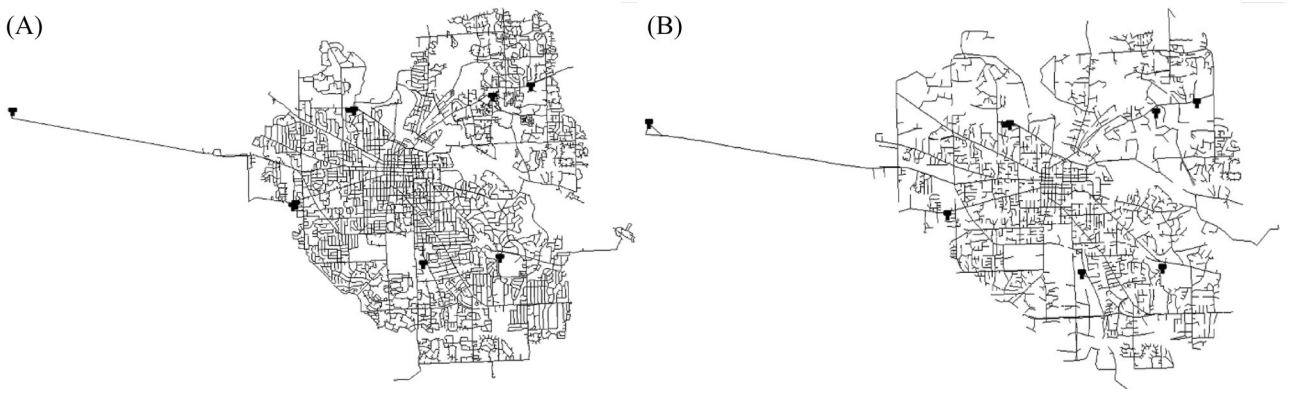


FIGURE 4 Water distribution network for (A) the real and (B) our synthetic system.

TABLE 1 Topological metric comparison between the real and our synthetic WDS.

WDS	Average nodal degree	Proportion of terminal nodes	Average betweenness centrality	Average distance to WTP (m)
Real	2.2	17.50%	0.005	5221
Synthetic	2.1	25.90%	0.013	5049

4.2 | Network validation

It is crucial to compare our synthetic WDS with the existing WDS to verify that it reflects the key properties of the existing system. As part of our analysis, we conducted topological and hydraulic assessments to validate our layout and hydraulic models. In the layout validation, we analyzed topological metrics to identify similarities between our synthetic and the existing WDS. For the hydraulic validation, we evaluated the model's capacity to simulate pressures under normal operating conditions. The layout and hydraulic model validation provide greater confidence in their application to damage scenarios.

4.2.1 | Network similarity

To assess the similarities between the topology of the WDSs, we examined global network parameters such as average nodal degree, the proportion of terminal nodes, and the betweenness centrality, shown in Table 1. These parameters were selected as they are commonly used to represent network characteristics. In addition, we evaluate the average distance from each building to the nearest WTP, as a longer distance could increase the likelihood of pipe failures during a disruptive event.

The nodal degree indicates the number of links connected to a node. For example, a node with no connections has a nodal degree of 0, and terminal nodes have a nodal degree of 1. Our synthetic WDS has a higher proportion of terminal nodes than the existing system due to the removal of some loops in the network generation process. Notably, both systems display similar nodal degree distributions, with more

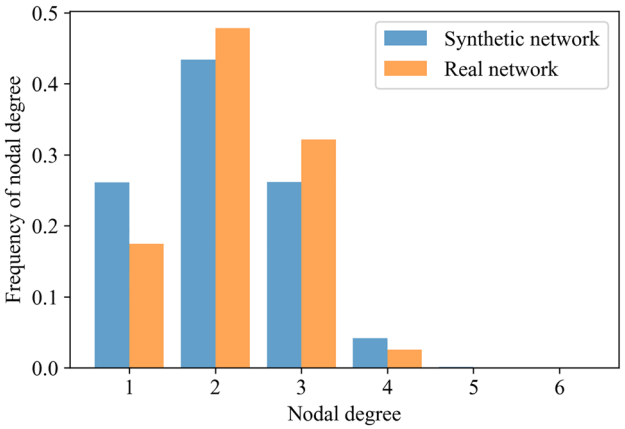


FIGURE 5 Nodal degree distribution for the real and our synthetic WDS.

than 43% of the nodes having a nodal degree of 2, as indicated in the average nodal degree results reported in Table 1. These results are illustrated in Figure 5.

The average betweenness centrality is a metric that measures the fraction of shortest paths that intersect each node. Because the real WDS has a higher pipe density and redundancy, the average betweenness centrality is lower, indicating that a smaller proportion of the shortest paths intersect each node. This observation is consistent with the fact that more redundant networks provide alternative pathways for the water flow, reducing the importance of individual nodes as critical points in the network.

We followed a two-step process to determine the distance between each building and the nearest WTP. First, we assigned each building to the nearest node based on Euclidean distance. Then, we calculated the shortest network path from the building's assigned node to the WTP. Our results indi-

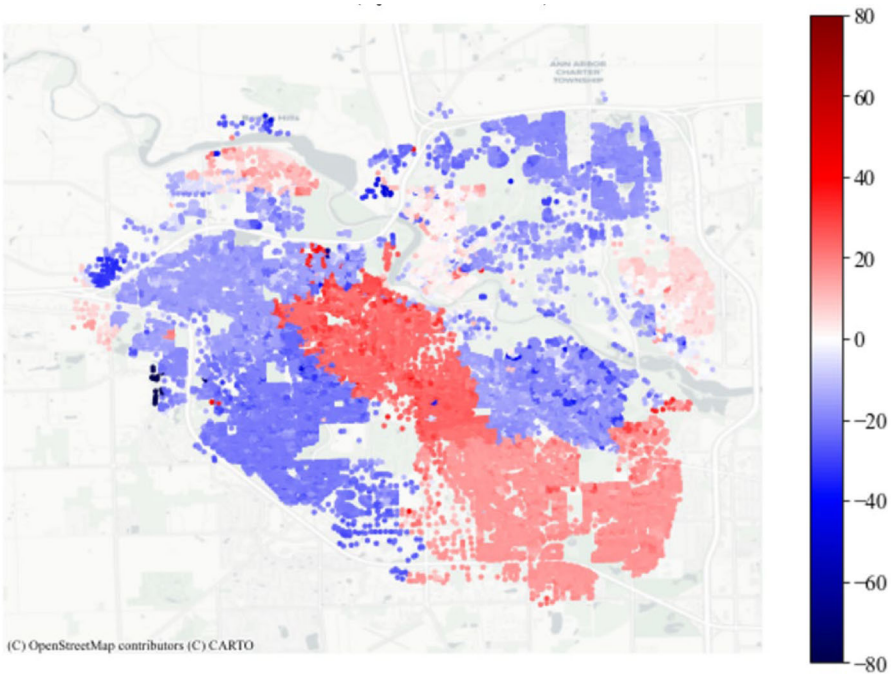


FIGURE 6 Average daily pressure differences at the building level between our synthetic and the real WDS in Ann Arbor, MI (synthetic–real).

cate that the real WDS has a greater distance on average compared with the synthetic WDS. This result is expected as the current network generation methodology does not consider pipes that connect the distribution system directly to buildings.

4.2.2 | Hydraulic model performance

In this section, we assess the hydraulic behavior of our synthetic WDS by comparing it with the real WDS. Specifically, we evaluated the daily pressure estimates at the building level, assuming normal operating conditions. Furthermore, we compared the pressure zones generated by our synthetic network to the real pressure zones. The real WDS pressure data were obtained directly from the utility company's in-house detailed hydraulic model.

The building-level daily pressure estimates were obtained by assigning each building the pressures of the nearest node, as described in the hydraulic methodology section (3.2.2). Figure 6 presents the average daily pressure differences between our synthetic and the existing WDS at the building level. Every point on the graph represents a building; the color indicates whether the average daily pressure estimates for the synthetic WDS were higher (red) or lower (blue) than those of the real WDS. The 10th and 90th percentiles for the average daily pressure differences are −20 PSI and 23 PSI, respectively. These results indicate that, while not perfect, our model generates a synthetic system capable of producing building-level pressures comparable to the real system. It is worth noting that the real WDS pressures are based on an imperfect hydraulic model and may differ from the actual field measurements. The daily pressure comparison was also performed using the minimum and maximum daily pressures and obtained similar patterns (Figure 7).

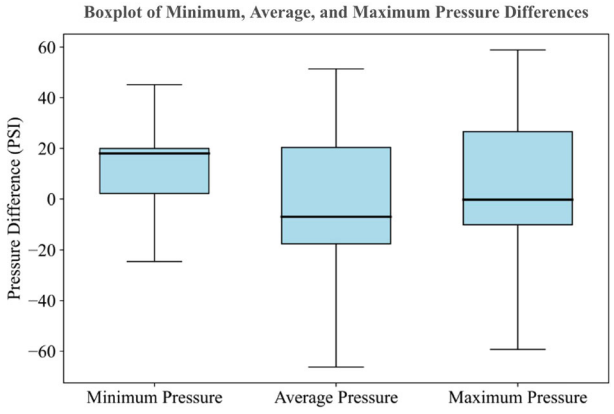


FIGURE 7 Boxplot for the minimum, average, and maximum daily pressure differences between our synthetic and the real WDS in Ann Arbor, MI.

The pressure differences could be explained by the fact that our synthetic model only includes pumps connecting tanks to water mains and does not include valves. Pumps are used throughout water systems to increase pressure at specific locations, especially when elevation differences are significant. Valves are commonly used in water systems to regulate water flow and are typically located at pressure zone boundaries, WTP(s), and tank locations. PRVs are used in practice to reduce high pressure in the system. Our synthetic model does not include PRVs, potentially accounting for some of the differences we see.

Figure 8 presents the pressure zones of the real and our synthetic WDS. As described in the hydraulic methodology

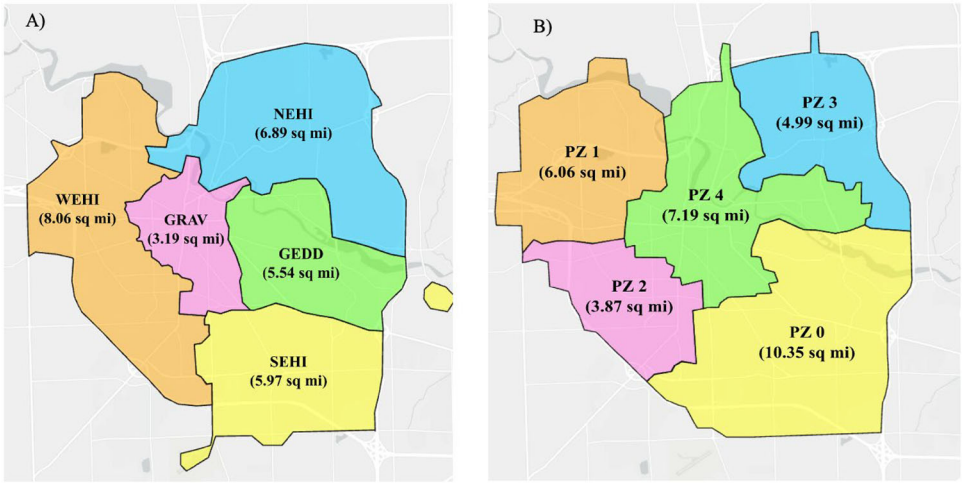


FIGURE 8 Pressure zone boundaries for (A) the real and (B) our synthetic WDS.

section (3.2.2), our model's node allocation into the different pressure zones minimizes pressure variations across the entire system. Our model does not consider the system's historical development; rather it is based on the most recent building and road conditions. However, in practice, as communities expand and water systems evolve, new components are added to the existing pressure zones based on the nodal pressure, elevation, and existing pressure zone boundaries. Consequently, the node allocation in our model may differ from the existing pressure zones but may represent a more efficient allocation based on the current system conditions.

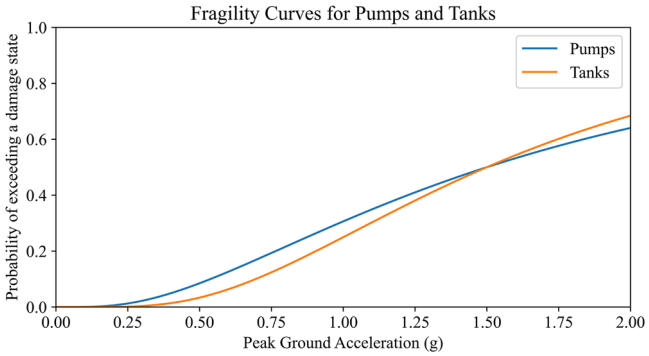


FIGURE 9 Fragility curves for pumps (blue) and tanks (orange).

4.3 | Earthquake scenario simulation

To demonstrate the applicability of our model, we simulated an earthquake's impact on the synthetic WDS. The simulation included the effects of pipe breaks, tank leaks, and pump failures caused by the earthquake. Other component failures, such as damage to reservoirs and WTP(s), were not included, but similar techniques can be used to model these failures. The fragility curve for pipes is based on the pipe's material and diameter. For each material-diameter combination, our model includes a fragility curve with a single damage state (DS) that indicates a pipe break (Kawashima et al., 1985). The tanks' single DS indicates a leak with a diameter of at least 0.25 meters (Figure 9A). The pumps' single DS indicates that it is not operational (Figure 9B). The fragility functions we used for pipes, tanks, and pumps are from ALA (American Lifelines Alliance, 2001b).

We conducted a convergence analysis to determine the number of replications required for our simulation to achieve a 95% confidence interval with a maximum width of 5%. Our analysis indicated that 500 replications are sufficient to achieve this level of precision. Figure 10 presents the results for 500 earthquake realizations of Richter scale magnitudes 5.0, 6.0, and 7.0. This graph indicates the proportion of nodes with pressures below 20 PSI for each hazard scenario.

The results indicate the magnitude 5.0 earthquake does not significantly damage the WDS. However, for a magnitude 6.0 earthquake, nodes closer to the epicenter and in isolated areas were more likely to experience low pressure. Nodes in isolated areas may be connected to the system by a single edge; therefore, if that critical edge is impacted, there is a high likelihood of low pressures. In the event of a magnitude 7.0 earthquake, over 65% of the nodes had a failure probability greater than 50%. The least-impacted pipes were those corresponding to the water mains, which is consistent with impacts to physical distribution lines as larger-diameter pipes tend to be more resistant to ground movements compared with smaller pipes.

Although the likelihood of earthquake scenarios occurring in Ann Arbor, MI is exceedingly low, the primary objective of our case study damage simulation was to demonstrate how our synthetic system could be used to assess the risk of water loss under various hazard scenarios. Other potential applications include the evaluation of restoration or reinforcement strategies. Additionally, it is important to note that a direct comparison between the simulated damage in our synthetic system and the actual system following the earthquake scenario was not conducted. The hydraulic data provided by

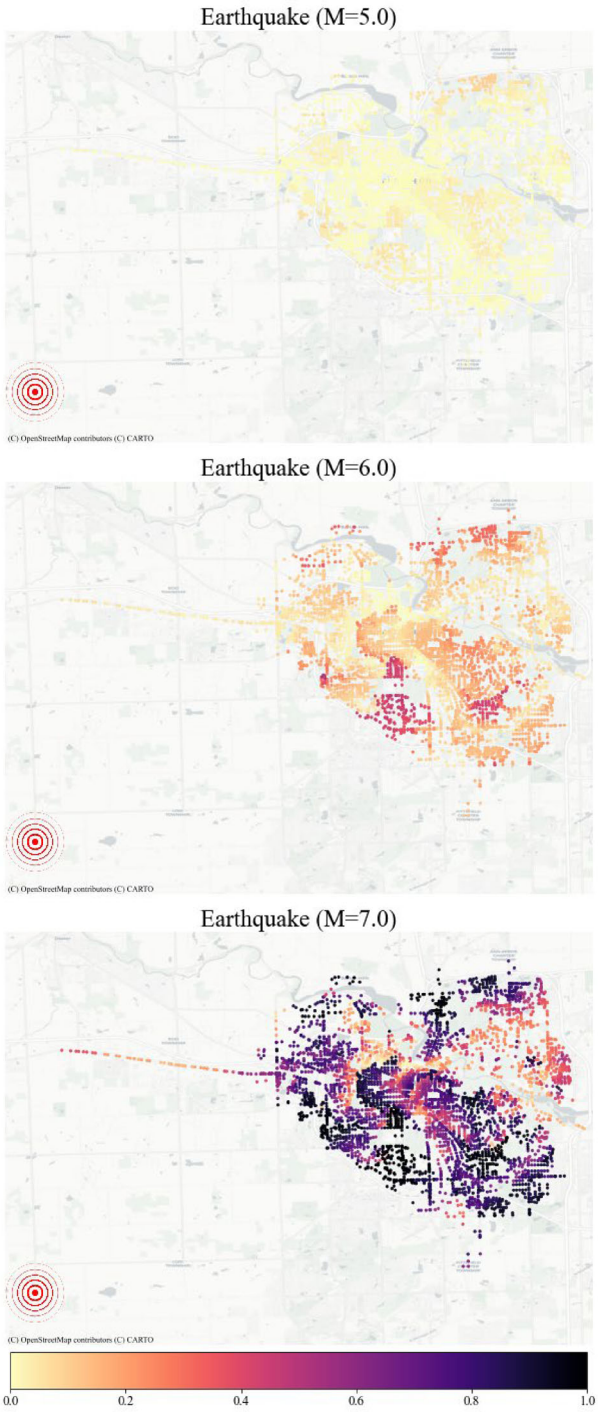


FIGURE 10 The proportion of nodes with pressures below 20 PSI in Ann Arbor, MI, for earthquakes of magnitude 5.0, 6.0, and 7.0. The red symbol represents the earthquake's epicenter at each map's southwest corner.

the utility company do not support such comparisons for a damaged system.

5 | CONCLUSION

We developed a model that uses publicly available data to generate a synthetic WDS given building data, locations of the water supply infrastructure, and road network. Our approach enables users to analyze the entire synthetic system or individual pressure zones, making it suitable for small- and large-scale systems. We evaluated our model using Ann Arbor, MI, by comparing our synthetic system with the existing WDS. The results indicate our synthetic system approximates the existing system's topological properties and hydraulic performance, producing building-level pressures reasonably close to those of the real system. To demonstrate one of the many applications of our model, we simulated the impact of various magnitude earthquakes on the synthetic WDS and evaluated the synthetic system's post-hazard performance. Although we focused on earthquakes, the damage model can be adapted to simulate the impact of other hazardous events if the necessary inputs, such as the hazard loading and component fragility functions, are provided.

Although our method provides a promising approach, it is important to note its limitations. The synthetic WDS we develop is representative of a real-life water system in the United States; due to different design guidelines, some assumptions may no longer apply in other countries. Furthermore, data collection may be challenging if building data or critical component locations, such as WTP(s) and tanks, are not publicly available. Additionally, our model assumes there is sufficient water supply for the entire system and does not consider external events, such as droughts, that affect the system's hydraulic performance during normal operating conditions. Furthermore, our system does not consider potential damage to water supply sources which may lead to overestimating the system's resilience.

Future refinement to our model could include improving the water demand estimates, developing pump allocation algorithms, and incorporating valves. If available, more detailed information on buildings, such as square footage and the number of floors, could be included to improve the water demand estimates at the building level as it provides information that can be used as a proxy for a more accurate consumption pattern. Additionally, the model could implement an optimization algorithm for pump allocation to improve pressure estimates in the system. Furthermore, incorporating multiple types of valves, such as PRVs, allows for simulating changes in the system's operational conditions following a hazard event.

Overall, our model provides a novel approach for generating a synthetic WDS that closely replicates real-world water systems using publicly available data. This methodology was specifically designed to support the development of infrastructure resilience strategies by identifying the system's critical components and vulnerabilities. Furthermore, evaluating water serviceability at a building level pre- and post-hazard, provides communities with a more comprehensive understanding of their existing water systems' hydraulic performance and potential inequities within their water services. Ultimately, this model provides an alternative approach to model, analyze, and improve the resilience of water systems, particularly in situations where access to the existing system data is limited.

ACKNOWLEDGMENTS

This research was supported by a grant from One Concern, Inc. to the University of Michigan. The authors' views expressed in this paper are their own and do not necessarily represent those of the funding organization.

DECLARATION OF COMPETING INTEREST

The authors declare no known financial interests or personal relationships that could have influenced the research presented in this paper. One author (Guikema) holds an ownership stake in One Concern, Inc.; however, the University of Michigan's established procedures ensured the research's independence and objectivity.

DATA AVAILABILITY STATEMENT

The data that support the findings of this study are available from the corresponding author upon reasonable request.

REFERENCES

Ahmad, N., Chester, M., Bondank, E., Arabi, M., Johnson, N., & Ruddell, B. L. (2022). A synthetic water distribution network model for urban resilience. *Sustainable and Resilient Infrastructure*, *7*(5), 333–347. https://doi.org/10.1080/23789689.2020.1788230

American Lifelines Alliance. (2001a). *Seismic fragility functions for water systems part 2: Appendices*.

American Lifelines Alliance. (2001b). *Seismic fragility formulations for water systems part 1: Guideline*.

American Society of Civil Engineers. (2021). *Drinking water*. https://infrastructurereportcard.org/wp-content/uploads/2017/01/Drinking-Water-2021.pdf

Baag, C. E., Chang, S. J., Jo, N. D., & Shin, J. S. (1998). Evaluation of seismic hazard in the southern part of Korea. In *Proceedings of 2nd International Symposium on Seismic Hazards and Ground Motion in the Region of Moderate Seismicity* (pp. 31–50).

Cheung, P. B., Van Zyl, J. E., & Reis, L. F. R. (2005). Extension of EPANET for pressure-driven demand modeling in water distribution system. *Computing and Control for the Water Industry*, *1*(1), 311–16.

Cornell University. (2008). GIRAFFE user's manual version 4.2.

Earthquake Engineering Research Institute. (2014). *EERI special earthquake report: M 6.0 South Napa Earthquake of August 24, 2014*. http://learningfromearthquakes.org/2014-08-24-south-napa/images/2014_08_24_south_napa/pdfs/EERI_EQ_report/EERI-Special-Eq-Report-2014-South-Napa-versionOct19web.pdf

Environmental Policy Innovation Center. (n.d.). *Provisional water utility service area boundaries viewer*. https://www.policyinnovation.org/technology/water-utility-service-area-boundaries

Environmental Protection Agency. (2018). *Earthquake resilience guide for water and wastewater utilities*. https://www.epa.gov/sites/default/files/2018-02/documents/180112-earthquakeresilienceguide.pdf

Environmental Protection Agency. (2008). *Water-efficient single-family new home specification supporting statement*. https://www.epa.gov/sites/default/files/2017-02/documents/ws-specification-home-suppstatement-v1.0.pdf

Federal Emergency Management Agency. (2017). *Hazus: Estimated annualized earthquake losses for the United States*. https://www.fema.gov/sites/default/files/2020-07/fema_earthquakes_hazus-estimated-annualized-earthquake-losses-for-the-united-states_20170401.pdf

Fujiwara, O., & Li, J. (1998). Reliability analysis of water distribution networks in consideration of equity, redistribution, and pressure-dependent demand. *Water Resources Research*, *34*(7), 1843–1850. https://doi.org/10.1029/98WR00908

Germanopoulos, G. (1985). A technical note on the inclusion of pressure-dependent demand and leakage terms in water supply network models. *Civil Engineering Systems*, *2*(3), 171–179. https://doi.org/10.1080/02630258508970401

Giustolisi, O., Savic, D., & Kapelan, Z. (2008). Pressure-driven demand and leakage simulation for water distribution networks. *Journal of Hydraulic Engineering*, *134*(5), 626–635. https://doi.org/10.1061/(ASCE)0733-9429(2008)134:5(626)

Haklay, M., & Weber, P. (2008). OpenStreetMap: user-generated street maps. *IEEE Pervasive Computing*, *7*(4), 12–18. https://doi.org/10.1109/MPRV.2008.80

Herfort, B., Lautenbach, S., Porto de Albuquerque, J., Anderson, J., & Zipf, A. (2023). A spatio-temporal analysis investigating completeness and inequalities of global urban building data in OpenStreetMap. *Nature Communications*, *14*(1), 3985. https://doi.org/10.1038/s41467-023-39698-6

Kammouh, O., Cimellaro, G. P., & Mahin, S. A. (2018). Downtime estimation and analysis of lifelines after an earthquake. *Engineering Structures*, *173*, 393–403. https://doi.org/10.1016/j.engstruct.2018.06.093

Kawashima, K., Aizawa, K., & Takahashi, K. (1985). Attenuation of peak ground motions and absolute acceleration response spectra of vertical earthquake ground motion. *Doboku Gakkai Ronbunshu*, *1985*(362), 169–176. https://doi.org/10.2208/jscej.1985.362_169

Klise, K. A., Bynum, M., Moriarty, D., & Murray, R. (2017). A software framework for assessing the resilience of drinking water systems to disasters with an example earthquake case study. *Environmental Modelling and Software*, *95*, 420–431. https://doi.org/10.1016/j.envsoft.2017.06.022

Klise, K. A., Murray, R., & Haxton, T. (2018). An overview of the water network tool for resilience (WNTR). *1st International WDSA /CCWI 2018 Joint Conference*.

Klise, K., Hart, D., Moriarty, D., Bynum, M., Murray, R., Burkhardt, J., & Haxton, T. (2017). *Water network tool for resilience (WNTR) user manual*. https://doi.org/10.2172/1376816

Laucelli, D., Berardi, L., & Giustolisi, O. (2012). Assessing climate change and asset deterioration impacts on water distribution networks: Demand-driven or pressure-driven network modeling? *Environmental Modelling & Software*, *37*, 206–216. https://doi.org/10.1016/j.envsoft.2012.04.004

Laucelli, D., & Giustolisi, O. (2015). Vulnerability assessment of water distribution networks under seismic actions. *Journal of Water Resources Planning and Management*, 141(6). https://doi.org/10.1061/(asce)wr.1943-5452.0000478

Lee, K., & Cho, K. H. (2002). Attenuation of peak horizontal acceleration in the Sino-Korean Craton. *Proceedings of the Annual Fall Conference of Earthquake Engineering Society of Korea*.

Logan, T., Williams, T., Nisbet, A., Liberman, K., Zuo, C., & Guikema, S. (2019). Evaluating urban accessibility: leveraging open-source data and analytics to overcome existing limitations. *Environment and Planning B: Urban Analytics and City Science*, *46*(5), 897–913. https://doi.org/10.1177/2399808317736528

Mair, M., Rauch, W., & Sitzenfrei, R. (2014). Spanning tree-based algorithm for generating water distribution network sets by using street network data sets. *World Environmental and Water Resources Congress 2014*, 465–474. https://doi.org/10.1061/9780784413548.050

Mair, M., Sitzenfrei, R., Möderl, M., & Rauch, W. (2012). Identifying multi-utility network similarities. *World Environmental and Water Resources Congress 2012*, 3147–3153. https://doi.org/10.1061/9780784412312.315

Mair, M., Zischg, J., Rauch, W., & Sitzenfrei, R. (2017). Where to find water pipes and sewers? On the correlation of infrastructure networks in the urban environment. *Water*, *9*(2), 146. https://doi.org/10.3390/w9020146

McDonald, Y. J., Anderson, K. M., Caballero, M. D., Ding, K. J., Fisher, D. H., Morkel, C. P., & Hill, E. L. (2022). A systematic review of geospatial representation of United States community water systems. *AWWA Water Science*, *4*(1). https://doi.org/10.1002/aws2.1266

Möderl, M., Fetz, T., & Rauch, W. (2007). Stochastic approach for performance evaluation regarding water distribution systems. *Water Science and Technology*, *56*(9), 29–36. https://doi.org/10.2166/wst.2007.598

Möderl, M., Sitzenfrei, R., Fetz, T., Fleischhacker, E., & Rauch, W. (2011). Systematic generation of virtual networks for water supply. *Water Resources Research*, *47*(2). https://doi.org/10.1029/2009WR008951

Muranho, J., Ferreira, A., Sousa, J., Gomes, A., & Marques, A. S. (2012). WaterNetGen: an EPANET extension for automatic water distribution network models generation and pipe sizing. *Water Supply*, *12*(1), 117–123. https://doi.org/10.2166/ws.2011.121

Muranho, J., Ferreira, A., Sousa, J., Gomes, A., & Marques, A. S. (2014). Pressure-dependent demand and leakage modelling with an EPANET extension: WaterNetGen. *Procedia Engineering*, *89*, 632–639. https://doi.org/10.1016/j.proeng.2014.11.488

Muranho, J., Ferreira, A., Sousa, J., Gomes, A., & Marques, A. S. (2020). Pressure-driven simulation of water distribution networks: Searching for numerical stability. *Environmental Sciences Proceedings*, *2*(1), 48. https://doi.org/10.3390/environsciproc2020002048

Pathirana, A. (2011). EPANET2 desktop application for pressure-driven demand modeling. *Water Distribution Systems Analysis 2010*, 65–74. https://doi.org/10.1061/41203(425)8

Pittsburg Tank & Tower Group. (n.d.). *Elevated water storage tanks*. https://www.pttg.com/elevated-water-storage-tanks/

Romero, N., O'Rourke, T. D., Nozick, L. K., & Davis, C. A. (2010). Seismic hazards and water supply performance. *Journal of Earthquake Engineering*, *14*(7), 1022–1043. https://doi.org/10.1080/13632460903527989

Rossman, L. A., Woo, H., Tryby, M., Shang, F., Janke, R., & Haxton, T. (2020). *EPANET 2.2 user manual*. U.S. Environmental Protection Agency, EPA/600/R-20/133.

Shi, P., & O'Rourke, T. D. (2008). *Seismic response modeling of water supply systems*. Cornell University.

Sitzenfrei, R., Fach, S., Kinzel, H., & Rauch, W. (2010). A multi-layer cellular automata approach for algorithmic generation of virtual case studies: VIBe. *Water Science and Technology*, *61*(1), 37–45. https://doi.org/10.2166/wst.2010.782

Sitzenfrei, R., Möderl, M., Hellbach, C., & Rauch, W. (2011). Application of a stochastic test case generation for water distribution systems. *World Environmental and Water Resources Congress 2011*, 113–120. https://doi.org/10.1061/41173(414)12

Sitzenfrei, R., Möderl, M., & Rauch, W. (2010). WDS designer—A tool algorithmic generation of water distribution systems based on GIS data. *World Environmental and Water Resources Congress 2010*, pp. 4193–4204. https://doi.org/10.1061/41114(371)427

Sitzenfrei, R., Möderl, M., & Rauch, W. (2013). Automatic generation of water distribution systems based on GIS data. *Environmental Modelling and Software*, *47*, 138–147. https://doi.org/10.1016/j.envsoft.2013.05.006

Stoker, J., & Miller, B. (2022). The accuracy and consistency of 3D elevation program data: A systematic analysis. *Remote Sensing*, *14*(4). https://doi.org/10.3390/rs14040940

The White House. (2013). *Presidential policy directive: Critical infrastructure security and resilience*. https://obamawhitehouse.archives.gov/the-press-office/2013/02/12/presidential-policy-directive-critical-infrastructure-security-and-resil

Toland, J., & Wein, A. (2021). A simplified method for rapid estimation of emergency water supply needs after earthquakes. *Water*, *13*(19). https://doi.org/10.3390/w13192635

Wagner, J. M., Shamir, U., & Marks, D. H. (1988). Water distribution reliability: Simulation methods. *Journal of Water Resources Planning and Management*, *114*(3), 276–294. https://doi.org/10.1061/(ASCE)0733-9496(1988)114:3(276)

Wang, Y. (2006). *Seismic performance evaluation of water supply systems*. Cornell University.

Wang, Y., & O'Rourke, T. (2007). Characterizations of seismic risk in Los Angeles water supply system. *5th China-Japan-US Trilateral Symposium on Lifeline Earthquake Engineering*, 391–399.

Wu, Z. Y., Wang, R. H., Walski, T. M., Yang, S. Y., Bowdler, D., & Baggett, C. C. (2008). Efficient pressure-dependent demand model for large water distribution system analysis. *Water Distribution Systems Analysis Symposium 2006*, pp. 1–15. https://doi.org/10.1061/40941(247)39

Yoo, D. G., Jung, D., Kang, D., & Kim, J. H. (2017). Seismic reliability–based multiobjective design of water distribution system: sensitivity analysis. *Journal of Water Resources Planning and Management*, *143*(2). https://doi.org/10.1061/(ASCE)WR.1943-5452.0000727

Yoo, D. G., Jung, D., Kang, D., Kim, J. H., & Lansey, K. (2016). Seismic hazard assessment model for urban water supply networks. *Journal of Water Resources Planning and Management*, *142*(2), 04015055. https://doi.org/10.1061/(ASCE)WR.1943-5452.0000584

Yu, J.-Z., Whitman, M., Kermanshah, A., & Baroud, H. (2021). A hierarchical Bayesian approach for assessing infrastructure networks serviceability under uncertainty: A case study of water distribution systems. *Reliability Engineering & System Safety*, *215*, 107735. https://doi.org/10.1016/j.ress.2021.107735

Yu, Y. X., & Jin, C. Y. (2008). Empirical peak ground velocity attenuation relations based on digital broadband records. *14th World Conference on Earthquake Engineering*.

How to cite this article: Pagan-Cajigas, Z., Guikema, S., Otaduy-Ramirez, R., Woolley, V., Smith, K., Hu, T., & Chen, T. (2025). Water outage predictions for natural hazards using synthetic water distribution systems. *Risk Analysis*, *45*, 2116–2131. https://doi.org/10.1111/risa.70004